

Short Communication

Effect of *Acinetobacter* Sp. on Corrosion Behavior of 10MnNiCrCu Steel in Simulated Marine Environment

Husong Rong¹, Xiaodong Zhao^{1,*}, Zifei Zhao¹, Hongbin Sun¹, Qiang Fu¹, Rui Ding¹, Jie Yang^{1,**},
Weijie Fan², Fulai Xiao³

¹ School of Ocean, Yantai University, Yantai 264005, China

² Qingdao Branch of Naval Aeronautical Engineering Academy, Qingdao 266041, China

³ Shandong Nanshan Aluminum Co., Ltd., Yantai 265706, China

*E-mail: danielxdzhao@aliyun.com, kittyangj@163.com

Received: 22 February 2021 / Accepted: 9 April 2021 / Published: 30 April 2021

Metal materials are susceptible to corrosion and microbiologically influenced corrosion (MIC) is very common in marine environment, which refers to a kind of electrochemical corrosion induced by the bacteria and their metabolic activities. In this study, electrochemical methods and scanning electron microscopy (SEM) were used to study the corrosion behavior of 10MnNiCrCu steel influenced by *Acinetobacter* sp. in a simulated marine environment. Electrochemical measurement results showed that the capacitance arc radius and charge transfer resistance of 10MnNiCrCu steel in *Acinetobacter* system were larger than those in sterile system, and the corrosion current density was lower, indicating a better corrosion resistance in the presence of *Acinetobacter*. The corrosion morphology observation showed that a protective biofilm/corrosion product film formed on the surface of the 10MnNiCrCu steel, which hindered the charge transfer at the interface between the metal and the solution, thereby inhibiting the corrosion. However, during the corrosion process, the partial detachment of the film led to the formation of a galvanic cell and accelerated the corrosion to a certain extent.

Keywords: *Acinetobacter*; Biofilm; Microbiologically influenced corrosion (MIC); 10MnNiCrCu steel

1. INTRODUCTION

Microorganisms exist widely in ocean, soil and other environmental systems[1], and grow rapidly under suitable conditions. As microorganisms have a strong affinity for metals[2], the surface of metal materials exposed to the microbial environment is prone to contamination by microorganisms and complex corrosion problems, as is called microbiologically influenced corrosion (MIC). MIC refers to a destructive corrosion induced by the presence and activities of bacteria[3]. Microorganisms change the interface conditions between the metal and media, as well as the electrochemical reaction, which is the

basis of the corrosion process[4]. In an environment where microorganisms and metal materials coexist, microorganisms are capable of using metals for material and energy metabolism, and generating organic matter through production of biofilms and extracellular metabolism, thus accelerating or inhibiting the corrosion of metals by complex corrosion mechanisms[5]. The formation of biofilm in the water environment is the result of the comprehensive effect of organic and inorganic macromolecule adsorption, microbial growth, extracellular polymer(EPS), water flow and other factors[6]. These adsorbed macromolecules/EPS alter the surface properties by changing the charge, wettability and surface energy on the material surface, thereby promoting or inhibiting the material corrosion. Most microorganisms in natural environment exist in the form of biofilm. Therefore, the formation of biofilm can be regarded as a universal survival strategy for microorganisms[7-8]. Biofilm is an interface-related microbial colony embedded in a self-made organic polymer matrix[9], which contains molecules from bulk water and/or corrosion products of metal substrate.

Most laboratories have published reports of the corrosion of metal materials accelerated by bacteria due to the existence and activity of bacterial biofilms[10-12]. Zhou found that the biofilm of aerobic *Pseudomonas aeruginosa* on the surface of 2304 DSS was the main cause of accelerated corrosion[13]. Li showed that 2707 super duplex stainless steel had no resistance to MIC due to the existence of *Pseudomonas aeruginosa* biofilm[14]. Duan pointed out that the complex strain system of sulfate-reducing bacteria *Desulfovibrio* and iron-reducing bacteria *Clostridium* inhibited the corrosion of steel[15], while a single strain accelerated the corrosion. In addition, after the dense bacterial biofilm completely generated, *Bacillus subtilis* C2 had a significant inhibition on the corrosion of cold rolled steel[16]. These studies show different strains and the state of biofilms will affect the corrosion of metals.

Acinetobacter sp.(in short, *Acinetobacter* below) are obligate aerobic and grow only in aerobic environment. *Acinetobacter* in natural environment is mainly distributed in water and soil environment. Most *Acinetobacter* has metabolic diversity and grows easily in simple microbial culture media. Smooth dome colonies with a diameter of about 2 mm are generally found and most are pale yellow or gray[17]. As the dominant bacteria in the marine environment, *Acinetobacter* is accumulated in waters [18]. At present, the research on *Acinetobacter* is focused on mechanism of infectivity, pathogenicity and drug resistance in the medical field[19-21]. In addition, *Acinetobacter* has significant effects in the degradation of hydrocarbon pollutants. Di studied that the Tust-DM21 strain belonging to the genus *Acinetobacter* was a prospective petroleum-degrading strain for its strong degradability for alkanes[22], cyclic hydrocarbons and aromatic hydrocarbons. Liu found that the ryegrass-*Acinetobacter* system had a remediation effect on oil-contaminated soil[23]. In view of MIC, as biofilm changes the physical and chemical environment for microbial corrosion reactions, the effect of *Acinetobacter* on corrosion is related to the tendency of attachment of bacteria and formation of biofilm.

The 10MnNiCrCu steel is widely used in marine environment for its good mechanical properties and economy. The behavior of steel in the natural environment not only depends on the material properties and environmental corrosivity, but also on the possible microorganisms. Studies have shown that steel is prone to corrosion induced by microorganisms[24-25], and localized pits and crevices are the main locations of MIC[26]. The microorganisms and generated biofilm adhered to the steel surface is recognized as precursor of MIC[27-28]. Considering the widespread distribution of *Acinetobacter* in

coastal areas and its potential effect on the corrosion of ship hull materials, the mechanism of *Acinetobacter* on the corrosion behavior of 10MnNiCrCu steel was primarily studied in this work.

2 EXPERIMENTAL METHODS

2.1 Material

The material selected for the experiment is 10MnNiCrCu steel provided by a shipyard, and its main chemical composition is shown in Table 1. Two specifications, 10 mm × 10 mm × 10 mm and 10 mm × 10 mm × 2 mm, of specimens were used for corrosion morphology observation and electrochemical measurement. The samples used for electrochemical measurement were connected with copper wire and sealed in PVC pipe with epoxy resin. The exposed surface area of these samples is 1 cm². The samples used for morphology observation were 10mm × 10mm × 10mm cubes. Before the experiment, the surface of the sample was polished with 240 to 1200# sandpapers, then rinsed with distilled water and degreased with acetone. Then the samples were placed in a deoxygenation chamber and tested after UV disinfection for 30 minutes.

In this study, *Acinetobacter* was isolated from the soil near the Laizhou Bay and cultured aerobically in Luria-Bertani(LB) medium consisting of 10g peptone, 3g beef paste and 5g sodium chloride in 1L deionized water, and the pH was adjusted to (7.0 ± 0.2) with 1 mol/L NaOH. The medium was sterilized in a sterilizer at 121°C for 20 min. After cooled to room temperature, the purified and active *Acinetobacter* was inoculated into the sterile medium at a ratio of 1:150. The medium inoculated with *Acinetobacter* was cultured in the incubator at 25°C. The medium inoculated with *Acinetobacter* was used as the experimental group, and the sterile culture medium was used as the control group.

Table 1. The main chemical compositions of 10MnNiCrCu steel (wt%).

Element	C	Si	Mn	S	P	Ni	Cr	Cu	Ti	V
Content wt%	≤0.12	0.40~ 0.70	0.70~ 1.10	≤0.010	≤0.015	0.50~ 1.00	0.60~ 0.90	0.40~ 0.60	≤0.020	≤0.08

2.2 Growth curve

The turbidimetric method was used to determine the growth curve of *Acinetobacter*. The purified *Acinetobacter* was cultured in the incubator at 25°C for 7 days. After morphological observation with a biological microscope, according to the preset time gradient, the absorbance at the wavelength of 600nm was determined by UT-1810 ultraviolet visible spectrophotometer. The average value of three times was used as the characterization of the number of bacteria in a certain period.

2.3 Electrochemical measurement

The electrochemical measurement was carried out using a PARSTAT 2273 electrochemical workstation with a three-electrode system. The reference electrode used for the experiment was a saturated calomel electrode, the counter electrode was a square platinum sheet with an area of 1 cm², and the working electrode was 10MnNiCrCu steel. After the stabilization of open circuit potential(OCP), each impedance spectrum was measured in the frequency range of 10⁵ to 10⁻² Hz under sinusoidal excitation with an amplitude of 10 mV, and all electrochemical tests were performed at 25 ± 2°C. The EIS results were fitted and analyzed using a ZSimpWin software. After immersion for 7 days the polarization curves were tested with a scanning range of ±250 mV relative to the OCP, and a scanning rate of 0.33 mV/s. The resulting data were fitted and analyzed using a C-view software to determine the corrosion potential(E_{corr}) and corrosion current density(I_{corr}).

2.4 SEM observation

The 10MnNiCrCu specimens used for corrosion morphology observation were immersed in medium inoculated with bacteria and sterile medium for 7 days. After taking out, The specimens were immersed in a 4% glutaraldehyde solution for 15 minutes to fix the biofilm on its surface. Then a series of 25%, 50%, 75% and 100% ethanol solution were used for dehydration, each for 15 minutes, then dried in vacuum, sprayed with palladium, and observed using a scanning electron microscopy (SEM, JSM-7610F).

3. RESULTS AND DISCUSSION

3.1 Observation of *Acinetobacter*

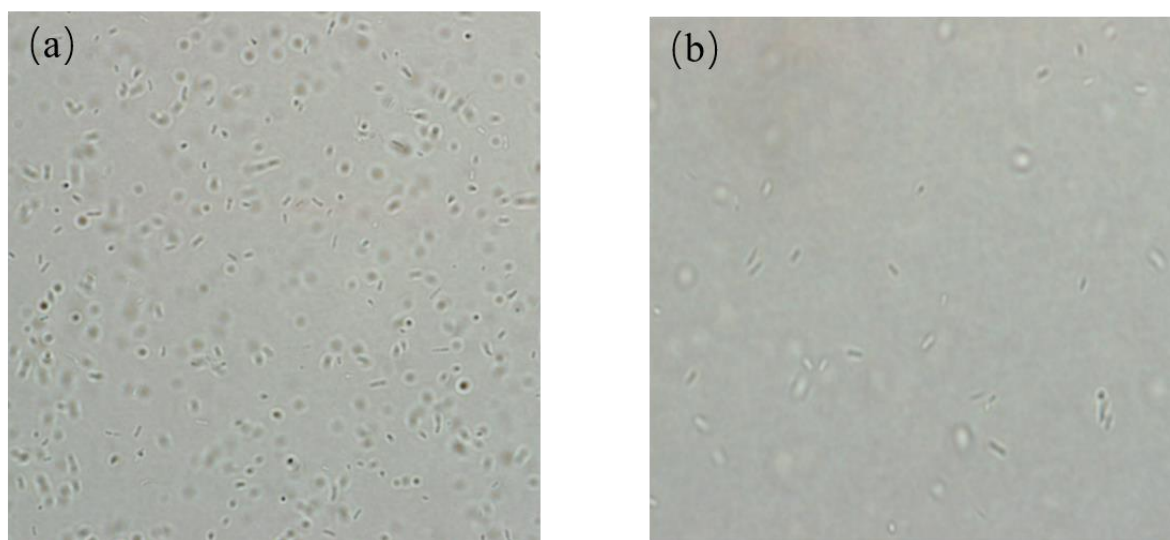


Figure 1. Morphology of *Acinetobacter* under a microscope with magnifications of (a) 400× (b) 1000×

Morphological observation of *Acinetobacter* was carried out with a biological microscope, as shown in Figure 1. The *Acinetobacter* is rod-shaped and active under the microscope. For its constant

activity, the morphology as shown in the figures is different. The longitudinal movement relative to the mirror of *Acinetobacter* shows a spherical shape, while the rod shape represents the lateral movement.

3.2 Growth curve

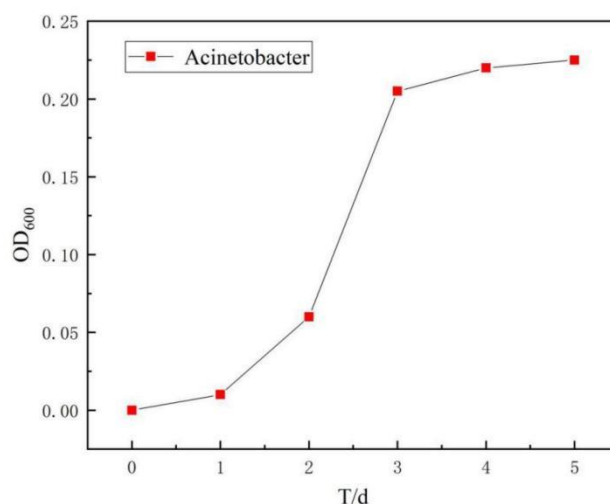


Figure 2. Growth curve of *Acinetobacter* in culture medium determined by OD₆₀₀ within 5 days

Figure 2 shows the measured OD₆₀₀ value of *Acinetobacter*, which represents the optical density absorbed by *Acinetobacter*. The higher the OD value, the more the bacteria. The 1st day was the lag phase of growth as the bacteria adapted to the new environment. The bacteria grew slowly and synthesized enzymes, coenzymes and other intermediate metabolites for later activities[29-30]. The following two days was the exponential growth phase of *Acinetobacter*. The activity of *Acinetobacter* increased and multiplied rapidly, and the number increased exponentially. The last two days was the stationary phase, as the reproduction rate of *Acinetobacter* gradually decreased, and the proliferation and death of bacteria reached a dynamic balance. At this stage, a large amount of metabolites accumulated in the solution.

3.3 EIS

EIS is usually used to study the electrochemical reactions at the metal/solution interface and the formation of corrosion products and biofilm in MIC[31-33]. Under stable OCP conditions, EIS tests were performed in sterile medium and *Acinetobacter* medium for 7 days, respectively. Figure 3 shows Nyquist and Bode diagrams of 10MnNiCrCu steels immersed in sterile and *Acinetobacter* systems for 7 days. As shown in the Nyquist diagram (Figure 3c), there are two time constants in the impedance spectrum of the *Acinetobacter* system, consisting of a high-frequency impedance loop and a low-frequency impedance loop. As seen from the Nyquist diagram, the radius of the capacitive arc under the two systems increased with the immersion time within 7 days (except the 6th day of the bacterial system).

The radius of the capacitive resistance arc is proportional to charge transfer resistance (R_{ct}) at the steel/solution interface.

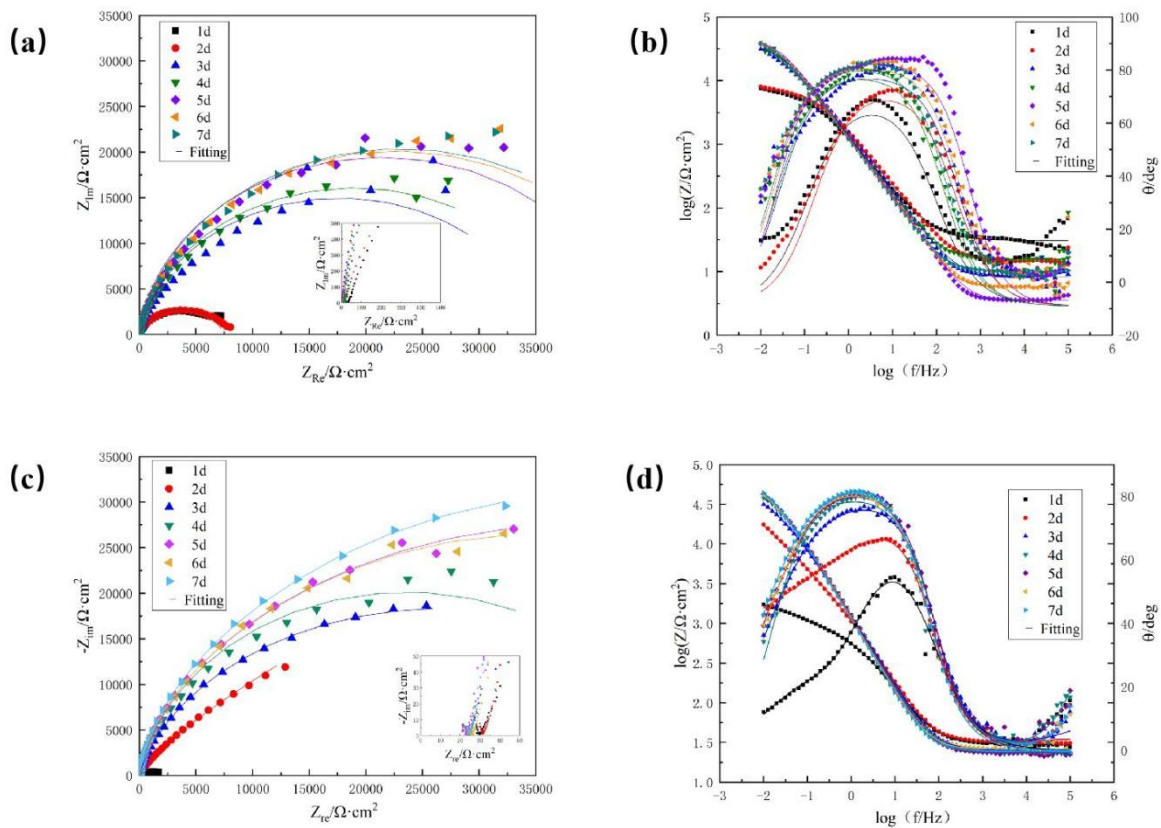


Figure 3. Nyquist and Bode diagrams of 10MnNiCrCu steel in (a), (b)sterile system and (c), (d)Acinetobacter system within 7 days

It indicated that the corrosion resistance of 10MnNiCrCu steel under the two systems was gradually increasing due to the biofilm/corrosion product film formed on the surface of the 10MnNiCrCu steel hindering the corrosive ions and thus inhibiting the corrosion. In addition, the dissolved organic substance in the culture medium might also adhere to the surface of the sample, preventing the penetration of Cl^- . Compared with the sterile system, the capacitive arc radius in the Acinetobacter system was generally larger than that in the sterile system except the first day, indicating that the presence of Acinetobacter inhibited the corrosion of 10MnNiCrCu steel. The impedance modulus in both systems increased at low frequencies with time of immersion, i.e, the corrosion rate of 10MnNiCrCu steel slowed down with the immersion time. It was consistent with the Nyquist results.

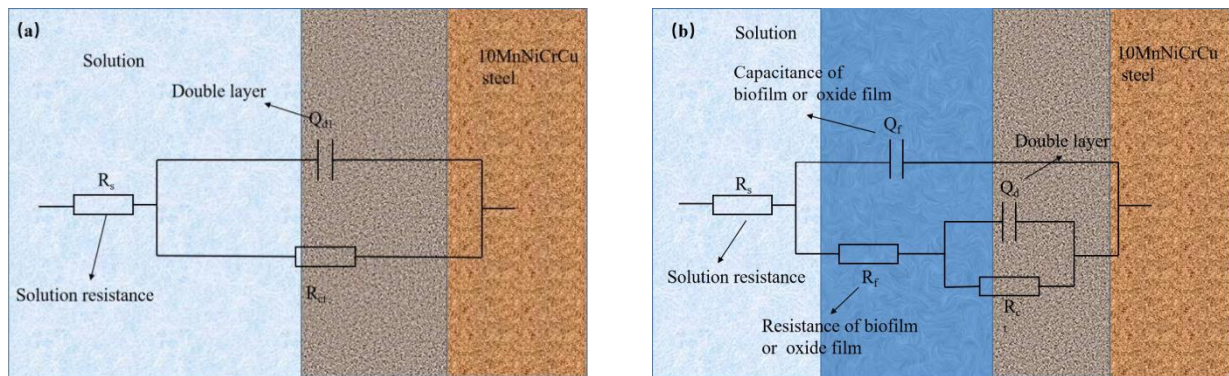


Figure 4. The equivalent circuit models used to fit the EIS data for 10MnNiCrCu steel immersed in (a) sterile system and (b) Acinetobacter system within 7 days

The equivalent circuit models shown in Figure 4 was used to fit the EIS data. R_s represents the solution resistance, Q_{dl} represents the electric double layer capacitance, Q_f represents the membrane capacitance, R_f represents the passivation film and biofilm resistance, R_{ct} represents the charge transfer resistance, and Q represents the constant phase component CPE (double-layer regular phase-angle component). CPE is determined by two parameters, namely the constant phase coefficient Y_0 and the dispersion coefficient n ($0 < n < 1$). ZsimpWin software was used for data fitting, and the results are shown in Table 2.

Table 2. Electrochemical impedance parameters of 10MnNiCrCu steels after different immersion time

Medium	Immersion time (d)	R_s ($\Omega \text{ cm}^2$)	$Q_f \times 10^{-4}$ (F cm^{-2})	n_f	R_f ($\Omega \text{ cm}^2$)	$Q_{dl} \times 10^{-4}$ (F cm^{-2})	n_{dl}	$R_{ct} \times 10^4$ ($\Omega \text{ cm}^2$)
Sterile	1	30.65	-	-	-	1.78	0.8105	0.7431
	2	14.33	-	-	-	1.29	0.8435	0.7400
	3	8.403	-	-	-	1.344	0.8972	3.2090
	4	15.75	-	-	-	1.405	0.8953	3.7920
	5	3.579	-	-	-	1.322	0.9414	4.2050
	6	5.758	-	-	-	1.467	0.9251	4.5270
	7	10.15	-	-	-	1.572	0.9207	4.6160
Acinetobacter	1	29.72	2.55	0.7986	813.7	22.49	0.6233	0.1204
	2	24.83	1.852	0.4841	8.985	1.005	0.9194	1.7420
	3	24.56	1.611	0.8761	23.36	1.423	0.8983	4.1510
	4	20.17	7.123	0.649	7.231	1.54	0.8979	4.7660
	5	23.33	1.502	0.9149	23.22	1.574	0.9030	5.6910
	6	26.16	1.554	0.9209	4.555	1.624	0.9091	5.5430
	7	24.7	1.592	0.9272	20.87	1.671	0.9141	6.2210

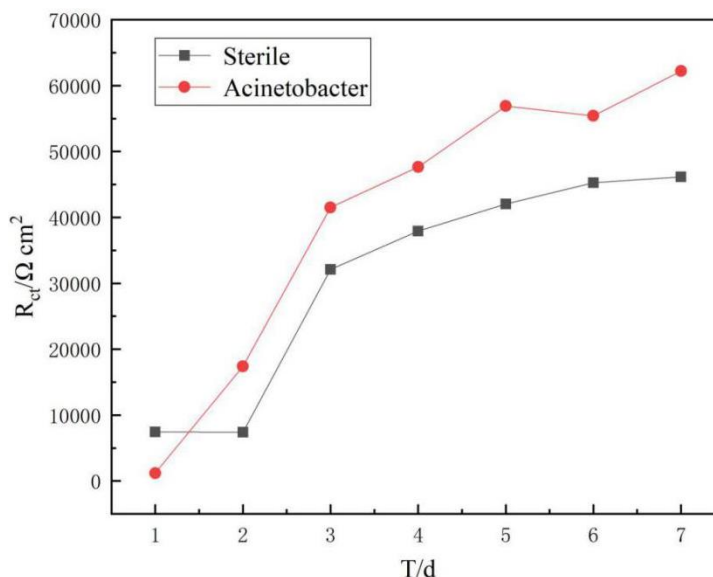


Figure 5. Variation of R_{ct} of 10MnNiCrCu steel within 7 days in sterile and Acinetobacter systems

The transfer of charge between the material surface and the solution is a process directly related to corrosion. In the sterile system and the Acinetobacter system, the charge transfer resistance was particularly small at the beginning, indicating a high corrosion rate. With the immersion time, the R_{ct} in both systems continued to increase, indicating that the corrosion rate slowed down with time. It was consistent with the impedance results. Except for the 1st day, the R_{ct} in the Acinetobacter system was greater than that in the sterile system generally, indicating that the presence of Acinetobacter inhibited the corrosion of 10MnNiCrCu steel. In the sterile system, R_{ct} increased from day 1 to day 7 except for the second day, showing that the corrosion rate of 10MnNiCrCu steel was gradually decreasing. With the immersion time, the corrosion products on the surface of the sample were accumulated and prevented the transport of corrosive media to the steel surface, thus reducing the corrosion rate. In the Acinetobacter system, with the immersion time, the biofilm/corrosion product film detached from the surface of the sample possibly, resulting in the decrease of R_{ct} in the Acinetobacter system on the 6th day. When two or more areas on the metal surface contacted with different concentrations of oxygen, the occurrence of oxygen concentration difference corrosion would accelerate the corrosion of the sample to a certain extent[34].

3.4 Polarization curve

Figure 6 shows the polarization curves of 10MnNiCrCu steel after immersion in sterile and Acinetobacter systems for 7 days. The polarization data is fitted with C-view software, and the relevant electrochemical parameters are shown in Table 3. The shapes of the polarization curves of the two systems were basically the same, indicating that the presence of Acinetobacter had not changed the electrochemical corrosion mechanism of 10MnNiCrCu steel, but only changed the corrosion rate. As shown in Table 3 that the corrosion current density of the 10MnNiCrCu steel in the Acinetobacter system was $0.8946\mu\text{A}/\text{cm}^2$, and that in the sterile system was $0.9889\mu\text{A}/\text{cm}^2$. It revealed that the corrosion rate of 10MnNiCrCu steel in Acinetobacter system was slower at this time. However, the corrosion potential

of the 10MnNiCrCu steel in the *Acinetobacter* system was more negative compared with that in the sterile system, indicating that the corrosion tendency of the steel in the *Acinetobacter* system was greater.

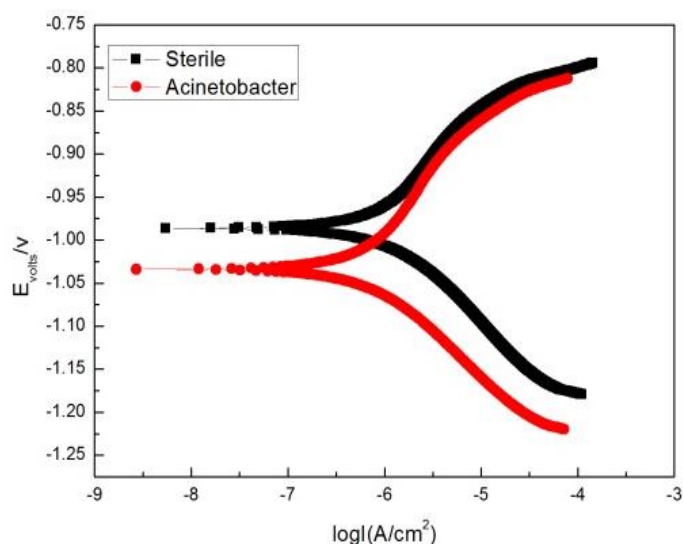


Figure 6. Polarization curves of 10MnNiCrCu steel immersed in sterile and *Acinetobacter* systems for 7 days

Table 3. Polarization curve fitting results of 10MnNiCrCu steel immersed in sterile and *Acinetobacter* systems for 7 days

Condition	Sterile medium	<i>Acinetobacter</i> medium
$I_{\text{corr}}(\mu\text{A}/\text{cm}^2)$	0.988	0.894
$E_{\text{corr}}(\text{V vs. SCE})$	-0.986	-1.033
$B_a(\text{mV}/\text{dec})$	158	209
$B_c(\text{mV}/\text{dec})$	101	118
Corrosion rate (MPY)	45.795	41.422

3.5 Corrosion morphology

Figure 7 showed the surface morphology of 10MnNiCrCu steel after immersion in sterile system and *Acinetobacter* system for 7 days. As shown in Figure 7(a), the surface of the sample was covered with a layer of corrosion products and little amount of bacteria, and a certain degree of pitting corrosion occurred in the localized area. As for Figure 7(a), (b), and (c), a large number of *Acinetobacter* attached to the metal surface and formed a biofilm/corrosion product film with metabolites to cover the surface of the sample. This biofilm/corrosion product film was supposed to slow down the corrosion rate of 10MnNiCrCu steel. However, with the immersion time, the film gradually became uneven and incomplete, and partially detached from the steel surface. When there was a concentration difference on the surface of the specimen, the corrosion was inevitably accelerated to a certain extent and pitting

corrosion was induced on the surface of the metal substrate.

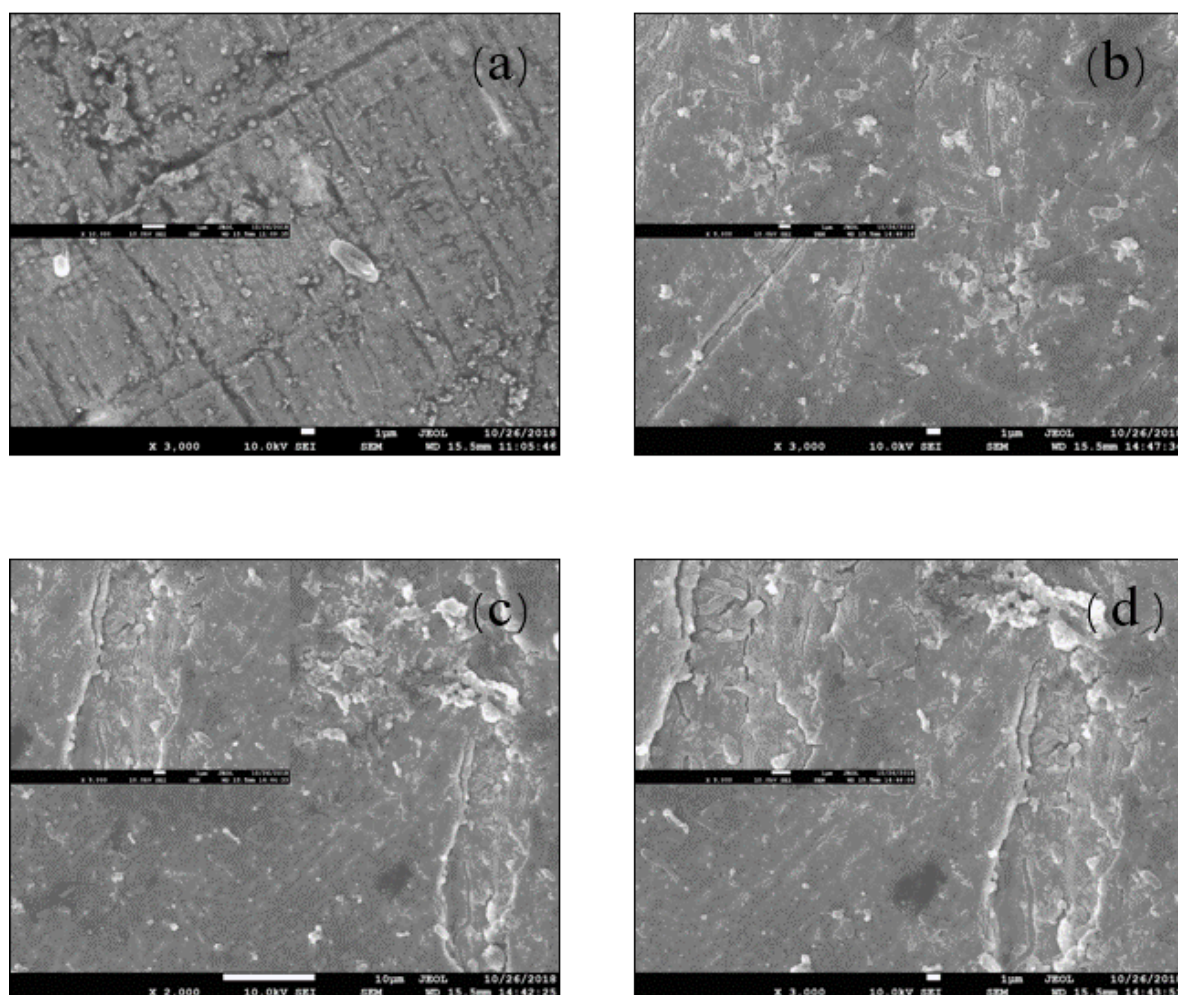


Figure 7. SEM images of surface morphology of 10MnNiCrCu steel immersed for 7 days in (a)sterile system and (b), (c), (d)Acinetobacter system with different magnifications.

4. DISCUSSION

Electrochemical impedance spectroscopy(EIS) is a non-destructive and effective method for studying the properties of metal surfaces and evaluating the protective performance of the film formed on the metal surface[35]. The radius(diameter) of the resistance arc, R_{ct} , and R_f are the key parameters for judging the corrosion rate. The higher the value of the three parameters, the greater the resistance between the metal and the environment interface, and the smaller the corrosion rate. In the sterile system, with the immersion time, the resistance arc radius and the R_{ct} value were continuously increasing, indicating that the corrosion rate of 10MnNiCrCu steel in the sterile system was gradually decreasing. There was no significant change in the characteristics of impedance spectroscopy. It was deduced that with the immersion time, the corrosion products accumulated on the surface of the sample hindering the penetration of corrosion ions and molecules to the steel surface[36-37]. In addition, the compactness of

the corrosion products on the steel surface in the sterile system might increase with the immersion time, resulting in the increase of the impedance modulus and decrease of the corrosion rate.

EIS results showed that there were two time constants in the *Acinetobacter* system. The time constant at high frequency corresponded to the biofilm/corrosion product film formed on the surface of the sample, and the time constant at low frequency corresponded to the charge transfer process of the electric double layer formed at the interface between the steel and the solution[38]. The capacitance arc of 10MnNiCrCu steel in *Acinetobacter* system increased with time. It was due to that the biofilm prevented the diffusion of corrosion products and inhibited the process of metal dissolution. In addition, the aerobic respiration of *Acinetobacter* consumed the oxygen and reduced the oxygen concentration on the electrode surface[6]. That is, the corrosion resistance of 10MnNiCrCu steel was slightly improved in the presence of *Acinetobacter* biofilm. Generally, biofilm can be a durable single-layer film at the metal/solution interface, hindering the transfer of charges between the cathode and anode[39], thereby inhibiting the corrosion of the metal.

As is seen from Table 3, the Tafel slope of the anode curve (B_a) in both systems was higher than that of the cathode curve (B_c), and the cathode Tafel slope (B_c) and anode Tafel slope (B_a) of the 10MnNiCrCu steel in *Acinetobacter* system were correspondingly greater than those in the sterile system. The current density of the sample in the *Acinetobacter* system was much smaller than that in the sterile system. It indicated that the cathodic and anodic reaction rates of 10MnNiCrCu steel in the *Acinetobacter* system were lower than those in the sterile system[40], as the metabolic activity of *Acinetobacter* inhibited the corrosion of 10MnNiCrCu steel. It is consistent with the impedance results.

The R_{ct} value of the steel in the *Acinetobacter* system increased rapidly in 1-3 days. At this time, the growth of *Acinetobacter* was in the exponential phase, and the reproduction and metabolism consumed a lot of oxygen. The decrease of the oxygen concentration on the electrode surface might slow down the corrosion of 10MnNiCrCu steel to a certain extent[6]. The increase in charge transfer resistance was attributed to the fact that the oxygen consumption of the biofilm controlled the cathodic reaction and the EPS protective layer prevented the surface oxidation[41]. With the immersion time, and the growth, reproduction, and metabolic activities of *Acinetobacter*, a layer of biofilm/corrosion product film generated on the surface of 10MnNiCrCu steel. The aerobic biofilm served as an oxygen barrier to slow down the penetration of oxygen and inhibit the corrosion[42]. However, the biofilm layer was composed of bacteria, water and EPS[43]. As the thickness of the biofilm continuously increased, while it gradually became uneven and incomplete[44]. This biofilm/corrosion product film partially detached from the surface gradually with the immersion time, and accelerated the corrosion of 10MnNiCrCu steel to a certain extent. The decrease in R_{ct} on the 6th day might be due to the unevenness of the biofilm induced the difference in oxygen concentration between the area covered by the biofilm and the area without it. The area with low oxygen concentration covered by biofilm served as the anode, and the area with high oxygen concentration without biofilm served as the cathode. Therefore, the uneven biofilm had a certain promotion effect on corrosion[45].

It can be seen from the Nyquist diagram and R_{ct} diagram that the resistance arc radius and R_{ct} of the 10MnNiCrCu steel in the *Acinetobacter* system were both larger than those in the sterile system within 7 days. It showed that the presence of *Acinetobacter* inhibited the corrosion of 10MnNiCrCu steel generally. Seen from the polarization curves, the corrosion current density of 10MnNiCrCu steel in the

Acinetobacter system was lower than that in the sterile system, and the polarization results were consistent with the impedance results.

5. CONCLUSIONS

In this study, the microbial growth curves, electrochemical impedance spectroscopy, polarization curves and surface morphology observation were used to study the effect of the Acinetobacter on the corrosion behavior and mechanism of 10MnNiCrCu steel. The growth and metabolism of Acinetobacter consumed oxygen on the metal surface, and the decrease of oxygen concentration inhibited the metal corrosion. EIS results and polarization curves showed that the presence of Acinetobacter inhibited the corrosion of 10MnNiCrCu steel, for the growth, reproduction and metabolic activities of Acinetobacter generated a dense biofilm/corrosion product film on the metal surface, thus preventing the penetration of corrosion ions and molecules into the metal substrate. However, with the immersion time, this protective film became uneven and incomplete, resulting in the difference in oxygen concentration between the area covered by the biofilm and without it. Thus a galvanic cell was formed and the corrosion was accelerated to a certain extent.

ACKNOWLEDGMENTS

The work is supported by State Key Laboratory of Ocean Engineering(Shanghai Jiao Tong University)(Grant No.1912) and the Green innovation science and technology plan of colleges and universities in Shandong Province (No.2020KJA014).

References

1. T. Y. Gu, R. Jia, T. Unsal and D. K. Xu, *J. Mater. Sci. Technol.*, 35(2019)631.
2. R. Jia, T. Unsal, D. K. Xu, Y. Lekbach and T. Y. Gu, *Int. Biodeterior. Biodegrad.*, 137(2019)42.
3. F. Mansfeld, *Electrochim. Acta*, 52(2007)7670.
4. I. B. Beech, *Encyclopedia of Environmental Microbiology*, (2003).
5. C. L. Yang and Q. C. Huang, *Chin. J. Infect. Control*, 11(2012)228.
6. S. Chongdar, G. Gunasekaran and P. Kumar, *Electrochim. Acta*, 50(2005)4665.
7. I. B. Beech and C. W. S. Cheung, *Int. Biodeterior. Biodegrad.*, 35(1995)59.
8. J. W. Costerton, D. R. Caldwell and H. M. Lappinscott, *Annu. Rev. Microbiol.*, 49(1995)711.
9. W. M. Dunne, *Clin. Microbiol. Rev.*, 15(2002)155.
10. L. Dijkshoorn, A. Nemec and H. Seifert, *Nat. Rev. Microbiol.*, 5(2007)939.
11. D. Landman, J. M. Quale, D. Mayorga, A. Adedeji, K. Vangala, J. Ravishankar, C. Flores and S. Brooks, *Arch. Intern. Med.*, 162(2002)1515.
12. S. Magnet, P. Courvalin and T. Lambert, *Antimicrob. Agents Chemother.*, 45(2001)3375.
13. E. Zhou, H. Li, C. Yang, J. Wang, D. Xu, D. Zhang and T. Gu, *Int. Biodeterior. Biodegrad.*, 127(2017)1.
14. H. Li, E. Zhou, D. Zhang, D. Xu, J. Xia, C. Yang, H. Feng, Z. Jiang, X. Li and T. Gu, *Sci. Rep.*, 6(2016)20190.
15. S. Wu, X. Zhang, G. Huang, M. Du and B. Hou, *Electrochim. Acta*, 54(2008)22.
16. Q. Qu, Y. He, L. Wang, H. Xu, L. Li, Y. Chen and Z. Ding, *Corros. Sci.*, 91 (2015)321.

17. P. Visca, H. Seifert and K. J. Towner, *IUBMB Life*, 63(2011)1048.
18. Y. H. Liu, H. Wang and X. K. Hu, *Microbiology China*, 43(2016)1579.
19. H. Liu, T. Gu, M. Asif, G. Zhang and H. Liu, *Corros. Sci.*, 114(2017)102.
20. F. Batmanghelich, L. Li and Y. Seo, *Corros. Sci.*, 121(2017)94.
21. D. K. Xu, Y. C. Li and T. Y. Gu, *Bioelectrochemistry*, 110(2016)52.
22. F. R. Di, D. H. Song, F. L. Liu and J. Yang, *Marin. Environ. Sci.*, 36(2017)898.
23. Y. J. Liu, Z. L. Cao, H. Y. Jia, Y. M. Zhao, W. Liu and W. Han, *Environ. Protec. Chem Ind.*, 38(2018)101.
24. A. LKH and B. HAV, *Int. Biodeterior. Biodegrad.*, 63(2009)891.
25. R. Javaherdashti, *Eur. J. Biol.*, 68(2009)65.
26. C. M. Xu, Y. H. Zhang, G. X. Cheng and W. S. Zhu, *Trans. Nonferrous Met. Soc. China*, 16(2006)299.
27. I. B. Beech, *Int. Biodeterior. Biodegrad.*, 53(2004)177.
28. B. J. Little, J. S. Lee and R. I. Ray, *Corrosion -Houston Tx-*, 62(2006)13.
29. S. Ray and V. C. Kalia, *Bioresour. Technol.*, 224(2016)743.
30. Y. Gu, X. Q. Lv and Y. F. Liu, *Metab. Eng.*, 51(2019)59.
31. S. J. Yuan, A. M. F. Choong and S. O. Pehkonen, *Corros. Sci.*, 49(2007)4352.
32. D. A. Miranda, S. A. Jaimes and J. M. Bastidas, *J. Solid State Electrochem.*, 18(2014)389.
33. F. Mansfeld, *Mater. Corros.*, 54(2003)489.
34. K. A. Zarasvand and V. R. Rai, *Int. Biodeterior. Biodegrad.*, 87(2014)66.
35. Y. Y. Shen, Y. H. Dong, Y. Yang, Q. H. Li, H. L. Zhu, W. T. Zhang, L. H. Dong and Y. S. Yin, *Bioelectrochemistry*, 132(2020)107408.
36. X. F. Zhai, J. Duan, J. Zhang, K. Li and B. R. Hou, *Surf. Coat. Technol.*, 316(2017)171.
37. S. Li, A. C. Bacco, N. Birbilis and H. Cong, *Corros. Sci.*, 112(2016)596.
38. J. Wu, W. Zhang, K. Chai and A. Yu, *Frontiers in Microbiology*, 11(2020)303.
39. H. A. Videla and L. K. Herrera, *Int. Biodeterior. Biodegrad.*, 63(2009)896.
40. H. Liu, X. Du, J. Duan, X. Zhai and B. Hou, *Corrosion Science and Protection Technology*, 28(2016)51.
41. K. M. Saleem, C. Yang, Y. Zhao and H. Pan, *Colloids Surf., B*, 189(2020)110858.
42. Y. Li, C. Chen, X. Li and R. Jia, *J. Mater. Sci. Technol.*, 34(2018)1713.
43. P. Stoodley, K. Sauer, D. G. Davies and J. W. Costerton, *Annu. Rev. Microbiol.*, 56(2002)187.
44. M. Hentzer and M. Givskov, *J. Clin. Invest.*, 112(2003)1300.
45. A. Abdolahi, E. Hamzah, Z. Ibrahim and S. Hashim, *Br. Corros. J.*, 50(2016)538.